New Agegraphic Dark Energy Model in Modified Symmetric Teleparallel Theory

Madiha Ajmal [*] and M. Sharif [†]

Department of Mathematics and Statistics, The University of Lahore, 1-KM Defence Road Lahore-54000, Pakistan.

Abstract

In this manuscript, we examine the cosmological significance of the new agegraphic dark energy model by investigating different cosmological parameters such as the equation of state parameter, $\omega_D - \omega'_D$ and the $r - s$ planes in the framework of $f(\mathcal{Q})$ theory. We consider flat Friedmann-Robertson-Walker universe model under interacting conditions between dark energy and dark matter. The equation of state parameter indicates a quintessence-like characteristic of the universe. The stability of the model is analyzed using the squared speed of sound parameter which demonstrates the unstable behavior of the new agegraphic dark energy model throughout the cosmic evolution. The freezing region is represented by the $\omega_D - \omega'_D$ plane, while the Chaplygin gas model corresponds to the $r - s$ plane. It is worthwhile to mention here that the interacting new agegraphic dark energy model addresses the cosmic coincidence problem by allowing the energy density ratio between dark energy and dark matter to evolve slowly over cosmic time.

Keywords: New agegraphic dark energy; $f(\mathcal{Q})$ gravity; Cosmological evolution.
PACS: 95.36.+x; 04.50.Kd; 64.30.+t.

[*]madihaajmal222@gmail.com
[†]msharif.math@pu.edu.pk

1 Introduction

The study of large-scale structures, supernova type-Ia and cosmic microwave background radiations have presented compelling evidences indicating that our universe is primarily characterized by two mysterious components, dark matter (DM) and dark energy (DE) [1]. Dark energy drives the current rapid expansion of the cosmos, while DM contributes to explain the rotation curves of galaxies and the overall structure of the universe. In the context of DE models, the rapid expansion has been discussed by altering the energy-momentum tensor (EMT) which is directly related to the right-hand side of the Einstein field equations. The modified theory of gravity involves altering the geometric aspect on the left-hand side of the field equations. Therefore, we are still a long way from creating a complete theory that can explain not only the rapid expansion of the universe but also problems with early cosmology, structure development, DM and other difficulties. Regardless of this approach, it is essential to include quantum effects to develop a precise theory of gravity. The quantum gravitational theory is the theory of gravity that includes the ideas of quantum mechanics. While quantum gravity remains an unresolved theory, several ideas have been suggested based on its principle. Holographic DE (HDE) and agegraphic DE (ADE) have been proposed as possible candidates for explaining the recent accelerated expansion of the universe by incorporating key properties of quantum gravity. The DE models offer a comprehensive framework for understanding the universe and solving various challenges in modern cosmology such as the coincidence problem [2].

The ADE framework originates from quantum mechanics based on the uncertainty principle and it incorporates gravitational implications in general relativity (GR). This model considers changes in spacetime and the content of matter to explain DE as determined by the universe. Cai [3] first introduced the original ADE model to study the rapid expansion of the cosmos. The expression for energy density, $\rho_D = 3n^2 M_p^2 T^{-2}$, includes the age ($T$) of the cosmos, M_p^2 is the Planck mass and the numerical value $3n^2$ is used to accommodate for some uncertainties. However, this framework has certain limitations that cannot be explained by the matter-dominated era of the universe. Wei and Cai [4] proposed a novel framework in the form of the new ADE (NADE) model, which replaces the age of the universe with conformal time. The coincidence problem is naturally solved by this model [5].

Recent interest in cosmology has focused on the reconstruction scenario

2

involving different DE models. Setare [6] explored the NADE model in $f(\mathcal{R})$ gravity ($\mathcal{R}$ is the Ricci scalar) and found evidence about the possible existence of the universe with phantom-like characteristics. Jamil and Saridakis [7] proposed the NADE model in the context of Horava-Lifshitz gravity, demonstrating its consistency with observations regarding the rapid expansion of the cosmos. Li et al. [8] investigated the behavior of the NADE as a rolling tachyon to examine its both potential and dynamics as a scalar field. Zhang et al. [9] studied the cosmic evolution of the NADE model with interaction between DE and matter component through statefinder parameter. Houndjo and Piattella [10] analyzed the numerical reconstruction of the $f(\mathcal{R}, \mathcal{T})$ gravity ($\mathcal{T}$ represents the trace of the EMT) that shows the features of HDE models. They examined the HDE and NADE models and constructed the corresponding $f(\mathcal{R}, \mathcal{T})$ gravity model as an alternative representation without the need for additional DE components.

Sharif and Jawad [11] investigated the mysterious characteristics of HDE and NADE models in the framework of GR. Fayaz et al. [12] used a Bianchi type-I cosmological model in the framework of reconstructed $f(\mathcal{R}, \mathcal{T})$ gravity to investigate the phantom and quintessence phases of cosmic evolution in HDE and NADE models. Setare et al. [13] computed the perturbed quantities for the NADE model and evaluated the results of the standard cold DM (CDM) model. Sharif and Saba [14] examined the cosmic dynamics of the reconstructed models using the phase planes and the cosmic diagnostic parameters. Pourbagher and Amani [15] analyzed the cosmological parameters and found that the total entropy variation increases as time progresses under thermodynamic equilibrium for specific free parameters in NADE model with $f(\mathcal{T}, \mathcal{B})$ theory, where $\mathcal{B}$ is boundary term.

The concept of GR is based on Riemannian geometry and asserts that the affine connection on the spacetime manifold must align with the metric, known as the Levi-Civita connection [16]. However, there can exist multiple options for an affine connection on any manifold. It is theoretically viable to explore gravitational theories using non-Riemannian geometry in which the curvature, torsion, and non-metricity all have non-zero values. When choosing a connection for which both curvature as well as non-metricity disappear, but allowing for some variation in torsion, it becomes feasible to formulate the teleparallel equivalent of GR [17]. Considering a flat spacetime manifold without torsion but with a non-zero nonmetricity, the symmetric teleparallel formulation of GR is obtained [18]. The f-theories are a category of modified theories and $f(\mathcal{R})$ gravity is focused on the Ricci scalar of the Levi-

3

Table 1: Classification of spacetimes

Relations	Spacetimes	physical representations
$\mathcal{Q}_{\zeta\xi} = 0,\ \mathbb{T} = 0,\ \mathcal{R}_{\zeta\xi} = 0$	Minkowski	Special Relativity
$\mathcal{Q}_{\zeta\xi} = 0,\ \mathbb{T} = 0,\ \mathcal{R}_{\zeta\xi} \neq 0$	Riemannian	General Relativity
$\mathcal{Q}_{\zeta\xi} = 0,\ \mathbb{T} \neq 0,\ \mathcal{R}_{\zeta\xi} = 0$	Weitzenbock	Teleparallel Gravity
$\mathcal{Q}_{\zeta\xi} \neq 0,\ \mathbb{T} = 0,\ \mathcal{R}_{\zeta\xi} = 0$		Symmetric Teleparallel
$\mathcal{Q}_{\zeta\xi} \neq 0,\ \mathbb{T} = 0,\ \mathcal{R}_{\zeta\xi} \neq 0$	Riemann-Weyl	Einstein-Weyl
$\mathcal{Q}_{\zeta\xi} = 0,\ \mathbb{T} \neq 0,\ \mathcal{R}_{\zeta\xi} \neq 0$	Riemann-Cartan	Einstein-Cartan
$\mathcal{Q}_{\zeta\xi} \neq 0,\ \mathbb{T} \neq 0,\ \mathcal{R}_{\zeta\xi} \neq 0$	Non-Riemannian	Einstein-Cartan-Weyl

Civita connection. The $f(\mathbb{T})$ [19] and $f(\mathcal{Q})$ [20] theories of gravity ($\mathbb{T}$ and $\mathcal{Q}$ represent the torsion scalar and non-metricity, respectively) address the curvature-less Weitzenböck connection. The $f(\mathcal{R})$, $f(\mathbb{T})$, and $f(\mathcal{Q})$ theories represent entirely different gravitational frameworks each typically offering a unique gravitational evolution. All three theories have shared the features in which each enables a mini-superspace depiction in the study of cosmology. For a non-linear function, the theory of gravity described by $f(\mathcal{R})$ is the fourth-order, while the $f(\mathbb{T})$ and $f(\mathcal{Q})$ theories are of the second-order.

Consequently, the existence of a scalar field resulting from the higher-order derivatives ($f(\mathcal{R})$ gravity) raised the degree of freedom, which results in the theory being equal to a scalar-tensor theory. We analyze the $f(\mathcal{Q})$ theory, an extension of the symmetric teleparallel GR (STGR) where gravity arises from the non-metricity. The theory is motivated by the need to explore its various underlying factors including theoretical consequences, consistency with observed data and its significance in cosmic contexts. This theory investigates theoretical effects based on cosmic domains and observational evidence. The metric tensor in $f(\mathcal{Q})$ theory has a non-zero covariant derivative which can be described using a new geometric variable called non-metricity. In non-Riemannian gravity, the field strengths include the non-metricity tensor $\mathcal{Q}_{\zeta\xi}$, torsion scalar $\mathbb{T}$ and curvature tensor $\mathcal{R}_{\zeta\xi}$. The classification of spacetimes and related theories are discussed in Table **1**.

Recent studies on $f(\mathcal{Q})$ gravity have uncovered cosmic challenges and observational limitations that can be used to demonstrate variations from the standard CDM model. Lu et al. [21] researched the cosmic properties in STGR and described that the universe's geometric nature contributes to

4

its accelerating expansion. Lazkoz et al. [22] studied the cosmic evolution using $f(\mathcal{Q})$ as polynomial functions of the redshift. Frusciante [23] proposed a particular model in this gravity. This model shared similarities with the ΛCDM model at a fundamental level.

Mandal and Sahoo [24] investigated the Hubble, Pantheon sample and the equation of state (EoS) parameters. The results of the standard CDM model are different from the $f(\mathcal{Q})$ model, which suggest quintessential behavior. Myrzakulov et al. [25] conducted a study on the cosmography of ghost DE and pilgrim DE in this theory. A recent investigation explored methods for parameterizing the effective EoS parameter in this context. Lymperis [26] analyzed the same theoretical framework to investigate the cosmological implications of the effective DE sector. Solanki et al. [27] found that the source of DE could be explained by the geometric expansion of GR. Koussour et al. [28] examined the properties of cosmic parameters in this gravity. In recent papers [29], we have developed generalized ghost DE and generalized ghost pilgrim DE models in the same gravity using the correspondence principle in a non-interacting framework. Additionally, we have examined the pilgrim and generalized ghost pilgrim DE models for the non-interacting scenario [30]. These models effectively replicate various cosmic epochs and align well with the latest observational data.

This paper uses the correspondence scheme to reconstruct the interacting case of the NADE $f(\mathcal{Q})$ model. Investigating the evolution of the universe involves studying the EoS parameter as well as analyzing the squared speed of sound and phase planes. The article is structured as follows. In section **2**, we give a summary of $f(\mathcal{Q})$ gravity and its significance for cosmological studies. In section **3**, the impacts of combined DE and CDM interaction are examined about the red-shift parameter. Furthermore, a method is employed to establish a link between NADE and $f(\mathcal{Q})$ gravity to devise a NADE $f(\mathcal{Q})$ model. The purpose of section **4** is to examine this model's evolution using cosmographic analysis. Our results are summarized in section **5**.

2   A Brief Overview of $f(\mathcal{Q})$ Gravity

In this section, assuming the properties of the affine connection essentially define a metric-affine geometry [31]. The gravitational potential can be considered as a value extended by the metric tensor $g_{\zeta\xi}$. In this particular context, a fundamental theorem in differential geometry asserts that the overall affine

connection can be broken down into three distinct and separate components [32]

$$\hat{\Gamma}^\lambda_{\zeta\xi} = \Gamma^\lambda_{\zeta\xi} + \mathcal{C}^\lambda_{\zeta\xi} + \mathcal{L}^\lambda_{\zeta\xi}, \tag{1}$$

where $\Gamma^\lambda_{\zeta\xi} = \frac{1}{2}g^{\lambda\sigma}(g_{\sigma\xi,\zeta} + g_{\sigma\zeta,\xi} - g_{\zeta\xi,\sigma})$ represents the Levi-Civita connection. The term $\mathcal{C}^\lambda_{\zeta\xi} = \hat{\Gamma}^\lambda_{[\zeta\xi]} + g^{\lambda\sigma}g_{\zeta\kappa}\hat{\Gamma}^\kappa_{[\xi\sigma]} + g^{\lambda\sigma}g_{\xi\kappa}\hat{\Gamma}^\kappa_{[\zeta\sigma]}$ denotes the contortion, characterized by the torsion tensor $\mathcal{T}^\alpha_{\zeta\xi} = 2\hat{\Gamma}^\alpha_{[\zeta\xi]}$, and lastly, the disformation $\mathcal{L}^\lambda_{\zeta\xi}$ is determined by

$$\mathcal{L}^\lambda_{\zeta\xi} = \frac{1}{2}g^{\lambda\sigma}(\mathcal{Q}_{\xi\zeta\sigma} + \mathcal{Q}_{\zeta\xi\sigma} - \mathcal{Q}_{\lambda\zeta\xi}), \tag{2}$$

which is expressed in relation to the non-metricity tensor $\mathcal{Q}_{\xi\zeta\sigma} = \nabla_\sigma g_{\zeta\xi} \neq 0$. This study will concentrate on a non-metric geometry which is characterized solely by its non-metricity tensor $\mathcal{Q}_{\xi\zeta\sigma}$, without any torsion or curvature. This innovative method has undergone many cosmological experiments and its investigation provided valuable understanding of the universe's late accelerated expansion. In the framework of different modified gravity theories, we start by considering the concept of extending $\mathcal{Q}$-gravity in a similar way as $f(\mathcal{R})$ theory has been generalized.

Considering the integral action of $f(\mathcal{Q})$ gravity as [18]

$$S = \int \left(\frac{1}{2k}f(\mathcal{Q}) + L_m \right) \sqrt{-g}d^4x, \tag{3}$$

while the matter lagrangian density is denoted by L_m, g represents the determinant of the metric tensor and $f(\mathcal{Q})$ represents an arbitrary function of $\mathcal{Q}$, which can be described as

$$\mathcal{Q} = -g^{\zeta\xi}(\mathcal{L}^\mu_{\nu\zeta}\mathcal{L}^\nu_{\xi\mu} - \mathcal{L}^\mu_{\nu\mu}\mathcal{L}^\nu_{\zeta\xi}). \tag{4}$$

Since the Levi-Civita connection in symmetric connections can be expressed in terms of the disfomation tensor as $\Gamma^\lambda_{\zeta\xi} = -\mathcal{L}^\lambda_{\zeta\xi}$, thus we have

$$\mathcal{L}^\lambda_{\zeta\xi} = -\frac{1}{2}g^{\lambda\sigma}(\nabla_\zeta g_{\sigma\xi} + \nabla_\xi g_{\sigma\zeta} - \nabla_\sigma g_{\zeta\xi}). \tag{5}$$

The superpotential can be defined as a function of $\mathcal{Q}$ given by

$$\mathcal{P}^\mu_{\zeta\xi} = -\frac{1}{2}\mathcal{L}^\mu_{\zeta\xi} + \frac{1}{4}(\mathcal{Q}^\mu - \tilde{\mathcal{Q}}^\mu)g_{\zeta\xi} - \frac{1}{4}\delta^\mu_{(\zeta}\mathcal{Q}_{\xi)}. \tag{6}$$

6

A different type of superpotential is described using Eq.(2) in (6) as

$$\mathcal{P}^{\mu\zeta\xi} = \frac{1}{4}\Big[-\mathcal{Q}^{\mu\zeta\xi} + \mathcal{Q}^{\zeta\mu\xi} + \mathcal{Q}^{\xi\mu\zeta} + \mathcal{Q}^{\zeta\mu\xi} - \tilde{Q}_\mu g^{\zeta\xi} + \mathcal{Q}^\mu g^{\zeta\xi} - \frac{1}{2}(\mathcal{Q}^\xi g^{\mu\zeta} + \mathcal{Q}^\zeta g^{\mu\xi}) \Big],$$

$$\mathcal{Q} = -\mathcal{Q}_{\mu\zeta\xi}\mathcal{P}^{\mu\zeta\xi} = -\frac{1}{4}(-\mathcal{Q}^{\mu\xi\rho}\mathcal{Q}_{\mu\xi\rho} + 2\mathcal{Q}^{\mu\xi\rho}\mathcal{Q}_{\rho\mu\xi} - 2\mathcal{Q}^\rho\tilde{\mathcal{Q}}_\rho + \mathcal{Q}^\rho\mathcal{Q}_\rho), \quad (7)$$

where

$$\mathcal{Q}_\mu = \mathcal{Q}_\mu{}^\zeta{}_\zeta, \quad \tilde{\mathcal{Q}}_\mu = \mathcal{Q}^\zeta{}_{\mu\zeta}. \tag{8}$$

Choosing $k = 1$ for simplicity gives the field equations of $f(\mathcal{Q})$ gravity, given as follows

$$\frac{-2}{\sqrt{-g}}\nabla_\zeta(f_\mathcal{Q}\sqrt{-g}P^\mu{}_{\zeta\xi}) - \frac{1}{2}fg_{\zeta\xi} - f_\mathcal{Q}(P_{\zeta\mu\nu}\mathcal{Q}_\xi{}^{\mu\nu} - 2\mathcal{Q}^{\mu\nu}{}_\zeta P_{\mu\nu\xi}) = \mathcal{T}_{\zeta\xi}, \quad (9)$$

where the EMT for matter is expressed by $\mathcal{T}_{\zeta\xi}$ and $f_\mathcal{Q} = \frac{\partial f(\mathcal{Q})}{\partial \mathcal{Q}}$.

3   Restructuring the NADE $f(\mathcal{Q})$ Model

In this section, we reconstruct the NADE $f(\mathcal{Q})$ gravity model through correspondence principle by using flat Friedmann-Robertson-Walker (FRW) universe model given as

$$ds^2 = -dt^2 + a^2(t)(dx^2 + dy^2 + dz^2), \tag{10}$$

where the scale factor is represented by $a(t)$. The EMT for a perfect fluid is defined as $\bar{\mathcal{T}}_{\zeta\xi} = (\rho_m + p_m)u_\zeta u_\xi + p_m g_{\zeta\xi}$, with ρ_m and p_m representing the thermodynamic energy density and isotropic pressure, respectively, u_ζ represents the the four-velocity field. We derive the Friedmann equations in $f(\mathcal{Q})$ gravity as

$$3H^2 = \rho_m + \rho_D, \quad 2\dot{H} + 3H^2 = p_m + p_D, \tag{11}$$

where the derivative with respect to t is indicated by an upper dot in the Hubble function $H = \frac{\dot{a}}{a}$. The density and pressure of the DE are provided as

$$\rho_D = \frac{f}{2} - 6H^2 f_\mathcal{Q}, \tag{12}$$

$$p_D = \frac{f}{2} + 2f_\mathcal{Q}\dot{H} + 2Hf_{\mathcal{Q}\mathcal{Q}} + 6H^2 f_\mathcal{Q}, \tag{13}$$

7

here Ω_D and Ω_m are the two fractional energy densities expressed as follows

$$\Omega_D = \frac{\rho_D}{\rho_{cr}} = \frac{\rho_D}{3H^2}, \quad \Omega_m = \frac{\rho_m}{\rho_{cr}} = \frac{\rho_m}{3H^2}, \tag{14}$$

one can represent 1 as the sum of Ω_D and Ω_m, where ρ_{cr} denotes the critical density.

Suppose the interplay between two fluid components, namely the DE and DM. As a result, when considering both fluids together, their respective energy densities do not individually remain constant but instead assume a specific form in the interacting scenario

$$\dot{\rho}_m + 3H(\rho_m + p_m) = \Gamma, \quad \dot{\rho}_D + 3H(\rho_D + p_D) = -\Gamma, \tag{15}$$

the interaction term in this case is denoted by Γ. It is clear that for energy transfer from DE to DM to occur, Γ must be positive. The value of Γ is simply determined as the product of H and ρ_D, since it is the inverse of time evolution. Here we take $\Gamma = 3\psi H(\rho_m + p_D) = 3\psi H\rho_D(1 + \chi)$ [25], where the coupling constant ψ indicates the strength of the interaction between DE and DM. By carefully examining the role of ψ, we have found that varying its value significantly influences the universe expansion rate, highlighting its critical role in cosmological evolution. Our results demonstrate how the interaction between these components affects the dynamics of the universe, emphasizing the importance of this factor in the broader analysis of cosmic evolution. The parameter χ is defined as

$$\chi = \frac{\rho_m}{\rho_D} = \frac{\Omega_m}{\Omega_D} = \frac{1 - \Omega_D}{\Omega_D}. \tag{16}$$

We can represent ω_D using the parameters that have been established previously [29]

$$\omega_D = -\frac{1}{2 - \Omega_D}\left(1 + \frac{2\psi}{\Omega_D}\right). \tag{17}$$

Substituting the age of the universe T with the conformal time η in the energy density of the ADE model, we obtain the energy density of the NADE model

$$\rho_D = \frac{3n^2 M_p^2}{\eta^2}, \quad \eta = \int \frac{dt}{a(t)},$$

where n is an arbitrary constant.

This model offers an alternative explanation to the accelerated expansion of the cosmos using the age of the universe as a measure of cosmic energy density. For simplification of subsequent calculations, we set $M_p^2 = 1$ and impose the restriction $n > 1$ to obtain

$$\rho_D = \frac{3n^2}{\eta^2}. \tag{18}$$

Taking the equivalent densities equal to each other, we demonstrate the connection between NADE and the $f(\mathcal{Q})$ gravity [33]. From Eqs.(12) and (18), it is clear that

$$\frac{f}{2} - 6H^2 f_{\mathcal{Q}} = \frac{3n^2}{\eta^2}. \tag{19}$$

This is the first-order linear differential equation in $\mathcal{Q}$ and its solution is

$$f(\mathcal{Q}) = c\sqrt{\mathcal{Q}} + \frac{12n^2}{\eta^2}, \tag{20}$$

where c represents the integration constant.

Now, we express this solution (20) in relation to the redshift parameter z. We represent the scale factor using a power-law formulation expressed as $a(t) = a_0 t^j$, where j and a_0 are arbitrary constants, with the current value of a_0 being equal to 1. The deceleration parameter is characterized by $q = -\frac{a\ddot{a}}{\dot{a}^2} = -1 + \frac{1}{j}$. Replacing the value of j in the function $a(t)$, we have

$$a(t) = t^{\frac{1}{1+q}}, \tag{21}$$

where $q = -0.832^{+0.091}_{-0.091}$ [34], with $q > -1$ indicating that the universe is expanding. This value reflects the acceleration of the universe at the present time. Utilizing this scale factor, we can express

$$H = (1+q)^{-1} t^{-1}, \quad H_0 = (1+q)^{-1} t_0^{-1}. \tag{22}$$

This suggests that q and H_0 are the parameters that determine the expansion of the universe. When we evaluate the connection between z and the scale factor, we obtain

$$H = H_0 \Psi^{1+q}, \quad \dot{H} = -H_0 \Psi^{2+2q}, \tag{23}$$

where $\Psi = 1 + z$. The value of $\mathcal{Q}$ is calculated by [29]
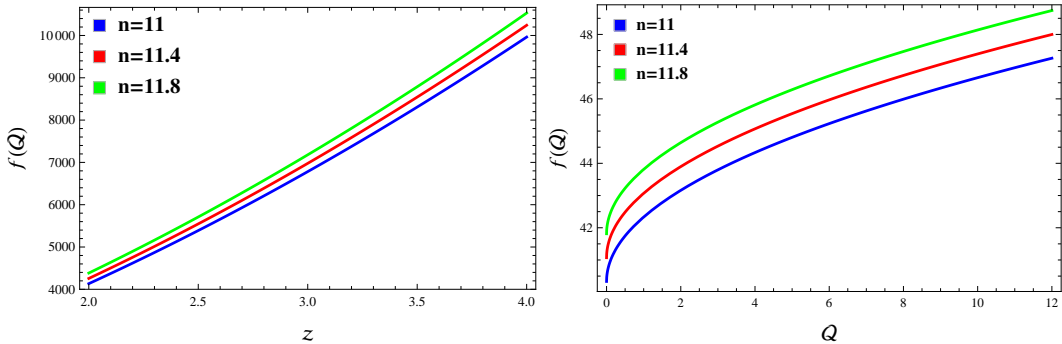
$$\mathcal{Q} = 6H^2.$$

Figure 1: Graph of $f(\mathcal{Q})$ against z and $\mathcal{Q}$.

Applying the value of H, we obtain

$$\mathcal{Q} = 6H_0^2\Psi^{2+2q}. \tag{24}$$

When we substitute this value in Eq.(20), We can express the solution in terms of z as follows

$$f(\mathcal{Q}) = \sqrt{6}c\sqrt{H_0^2\Psi^{2q+2}} + \frac{12n^2q^2\Psi^{2q}}{(q+1)^2}. \tag{25}$$

For the purpose of analysis, we use three fixed values of $n = 11, 11.4$ and 11.8 to explore the graphical behavior in the $f(\mathcal{Q})$ theory. If we change the value of n, it has a distinct impact on these graphical representations. These values were chosen to provide a close examination of the model's behavior under slight variations, allowing us to analyze the stability and consistency of the results. The behavior of the graphs with these values is favorable, as it leads to good representations in parametric graphs (phase-planes). We have considered the current value of the Hubble constant H_0 as $70Kms^{-1}Mpc^{-1}$, which is widely accepted based on recent observational data. This value is used throughout the analysis to ensure consistency in the calculated quantities. Any variation in the Hubble constsnt would influence the results, but our choice reflects the present-day accepted value from cosmological observations. Additionally, We arbitrarily set the constant of integration $c = 2$, which negligibly impacts the graphical behavior of the plots.

Figure **1** demonstrates that the reconstructed NADE model consistently stays positive and rises with both z and Q for all chosen values of n. We
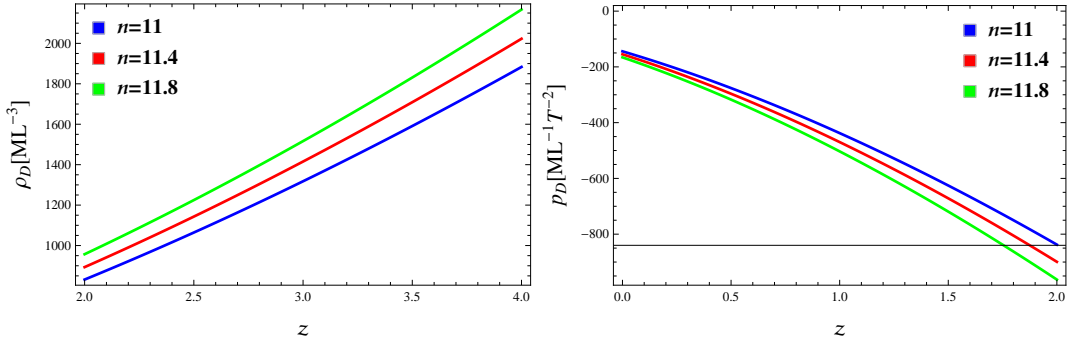
Figure 2: Graphs of ρ_D and p_D against z.

also examine the characteristics of ρ_D and p_D in the context of NADE reconstructed $f(\mathcal{Q})$ gravity model. Applying Eq.(20) to (12) and (13), we derive

$$\rho_D = \frac{6n^2}{\eta^2} - \frac{1}{2}c\left(\sqrt{6}H - \sqrt{\mathcal{Q}}\right),$$

$$p_D = \frac{c\eta^2\left(\mathcal{Q}(2\dot{H} - \mathcal{Q}) + 6H^2\mathcal{Q} - H\right) - 12n^2\mathcal{Q}^{3/2}}{2\eta^2\mathcal{Q}^{3/2}},$$

where $\sigma = q + 1$ for further simplification. In terms of redshift parameter, these equations take the following form

$$\rho_D = \sqrt{\frac{3}{2}}c\left(\sqrt{H_0^2\Psi^{2q+2}} - H_0\Psi^\sigma\right) + \frac{6n^2q^2\Psi^{2q}}{\sigma^2}, \qquad (26)$$

$$p_D = \left[q^2\Psi^{2q}\left\{-\left[\left(cH_0\sigma^2\Psi^{1-q}\left(12H_0^2\Psi^{3q+3} + 1\right)\right)\left(q^2\right)^{-1}\right]\right.$$

$$\left. - 72\sqrt{6}n^2\left(H_0^2\Psi^{2q+2}\right)^{3/2}\right\}\right]\left[12\sqrt{6}\sigma^2\left(H_0^2\Psi^{2q+2}\right)^{3/2}\right]^{-1}. \qquad (27)$$

Figure **2** shows how the reconstructed NADE $f(\mathcal{Q})$ gravity behaves with z. For all values of n, the reconstructed NADE $f(\mathcal{Q})$ gravity has an exponentially increasing ρ_D. The quantity p_D indicates a decreasing pattern and continuously shows negative behavior, which corresponds with the DE behavior.

11

4   Cosmographic Analysis

In this section, we perform cosmographic analysis on the EoS parameter and phase planes for the reconstructed NADE $f(\mathcal{Q})$ gravity model in an interacting scenario to investigate the universe evolution. We also explore ν_s^2 to analyze the stability of this model.

In this context, the negative values of the coupling constant were chosen because they provided consistent and meaningful results for the model we are exploring. While positive values can lead to changes in graphical behavior, they may not achieve the same level of consistency with observational data. As noted by Feng et al. [35], a small coupling constant is necessary to align with observations and addresses the coincidence problem. Our analysis shows that employing a small coupling constant, even if negative, helps avoid this problem while remaining compatible with current observations.

4.1   Equation of State Parameter

The equation of state parameter ($\omega_D = \frac{p_D}{\rho_D}$) for DE is essential in characterizing the cosmic inflation phase and the subsequent expansion of the cosmos. We study the condition for the universe undergoing acceleration, which happens when the EoS $\omega_D < -\frac{1}{3}$. When $\omega_D = -1$, it represents the cosmological constant. However, the cases $\omega_D = \frac{1}{3}$ and $\omega_D = 0$ denote radiation-dominated and matter-dominated eras, respectively. Furthermore, the phantom situation arises when $\omega_D < -1$, while $-1 < \omega_D < -\frac{1}{3}$ leads to quintessence phase of the universe expansion. Referring to Eq.(17), we can derive

$$
\begin{aligned}
\omega_D =\ & -\left\{\eta^2 \mathcal{Q}\left(\eta^2\left(\sqrt{6}cH - c\sqrt{\mathcal{Q}} + 2\mathcal{Q}\psi\right) - 12n^2\right)\right\}\left\{\left(\left(\sqrt{\mathcal{Q}} - \sqrt{6}H\right)\right.\right. \\
& \times\ \left.\left. c\eta^2 + 12n^2\right)\left(\eta^2\left(c(\sqrt{\mathcal{Q}} - \sqrt{6}H) - 2\mathcal{Q}\right) + 12n^2\right)\right\}^{-1},
\end{aligned} \qquad (28)
$$

while in the context of z, this is expressed as

$$
\begin{aligned}
\omega_D =\ & -\left[6H_0^2\sigma^2\Psi^2\left\{\left[\left(\sigma^2\left(12H_0^2\psi\Psi^{2q+2} - \sqrt{6}c\left(\sqrt{H_0^2\Psi^{2q+2}} - H_0\Psi^{q+1}\right)\right)\right.\right.\right.\right. \\
& \times\ \left.\left.\Psi^{-2q}\right)\left(q^2\right)^{-1}\right] - 12n^2\right\}\left[q^2\left\{\left[\left(\sqrt{6}\Psi^{-2q}\left(\sqrt{H_0^2\Psi^{2q+2}} - H_0\Psi^\sigma\right)\right.\right.\right.\right.
\end{aligned}
$$

12
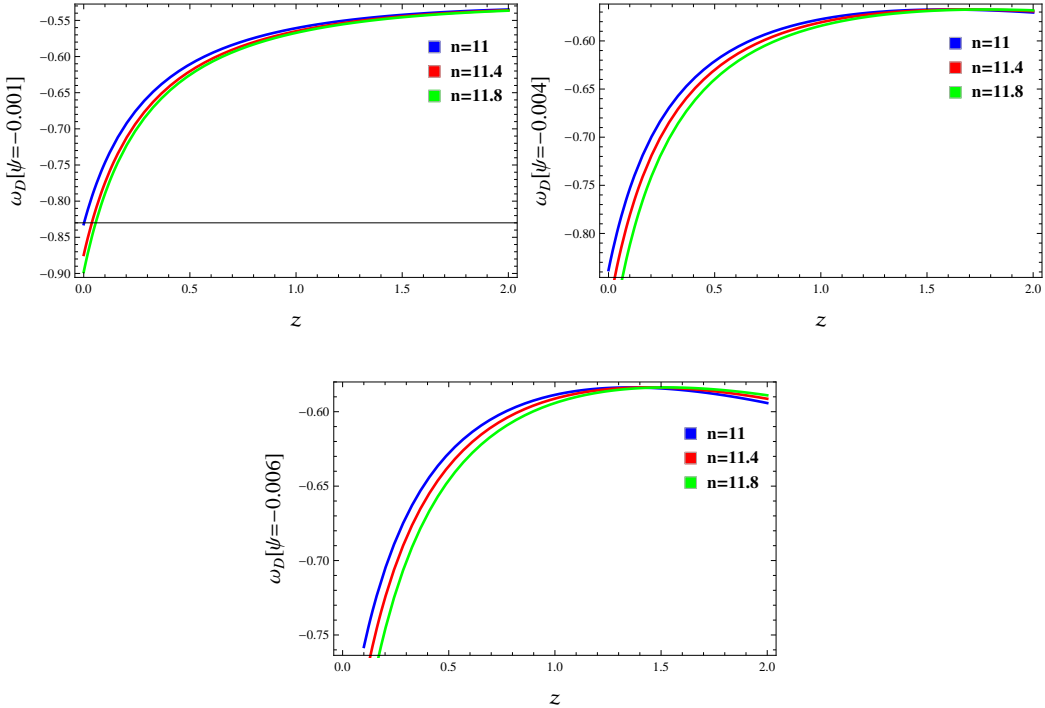
Figure 3: Plots of ω_D versus z.

$$\times \quad c\sigma^2\Big)\big(q^2\big)^{-1}\Big] + 12n^2\bigg\}\bigg\{12n^2 - \bigg[\bigg(\bigg(12H_0^2\Psi^{2q+2} - \sqrt{6}c\bigg(\sqrt{H_0^2\Psi^{2q+2}}$$

$$- \quad H_0\Psi^\sigma\bigg)\bigg)\sigma^2\Psi^{-2q}\Big)\big(q^2\big)^{-1}\bigg]\bigg\}\bigg]^{-1}.$$

Figure **3** demonstrates the dynamical evolution of EoS in the NADE $f(\mathcal{Q})$ gravity for various values of n and ψ. It exhibits values greater than -1 and less than $-\frac{1}{3}$, specifically expressed as $-1 < \omega_D < -\frac{1}{3}$. This suggests the presence of quintessence field DE in this model.

4.2 The $\big(\omega_D - \omega'_D\big)$-Plane

Here, we make use of the phase plane $\big(\omega_D - \omega'_D\big)$, where ω'_D represents the evolutionary behavior of ω_D and prime indicates the derivative with respect to $\mathcal{Q}$. Caldwell and Linder [36] introduced this cosmic framework to explore the quintessence DE paradigm, which can be divided into freezing $(\omega_D <$

0, $\omega'_D < 0$) and thawing ($\omega_D < 0$, $\omega'_D > 0$) scenarios. The current cosmic expansion model is represented by the freezing region, which indicates a more rapid phase in comparison to thawing region. Differentiating Eq.(28) with respect to $\mathcal{Q}$ gives us

$$
\begin{aligned}
\omega'_D &= -\frac{\eta^2\Big(\eta^2(\sqrt{6}cH - c\sqrt{\mathcal{Q}} + 2\mathcal{Q}\psi) - 12n^2\Big)}{\Big(c\eta^2(\sqrt{\mathcal{Q}} - \sqrt{6}H) + 12n^2\Big)\Big(\eta^2(c(\sqrt{\mathcal{Q}} - \sqrt{6}H) - 2\mathcal{Q}) + 12n^2\Big)} \\
&+ \frac{c\eta^4\sqrt{\mathcal{Q}}\Big(\eta^2(\sqrt{6}cH - c\sqrt{\mathcal{Q}} + 2\mathcal{Q}\psi) - 12n^2\Big)}{2\Big(c\eta^2(\sqrt{\mathcal{Q}} - \sqrt{6}H) + 12n^2\Big)^2\Big(\eta^2(c(\sqrt{\mathcal{Q}} - \sqrt{6}H) - 2\mathcal{Q}) + 12n^2\Big)} \\
&+ \frac{\eta^4\mathcal{Q}\Big(\frac{c}{2\sqrt{\mathcal{Q}}} - 2\Big)\Big(\eta^2(\sqrt{6}cH - c\sqrt{\mathcal{Q}} + 2\mathcal{Q}\psi) - 12n^2\Big)}{\Big(c\eta^2(\sqrt{\mathcal{Q}} - \sqrt{6}H) + 12n^2\Big)\Big(\eta^2(c(\sqrt{\mathcal{Q}} - \sqrt{6}H) - 2\mathcal{Q}) + 12n^2\Big)^2} \\
&- \frac{\eta^4\mathcal{Q}\Big(2\psi - \frac{c}{2\sqrt{\mathcal{Q}}}\Big)}{\Big(c\eta^2\Big(\sqrt{\mathcal{Q}} - \sqrt{6}H\Big) + 12n^2\Big)\Big(\eta^2\Big(c\Big(\sqrt{\mathcal{Q}} - \sqrt{6}H\Big) - 2\mathcal{Q}\Big) + 12n^2\Big)}.
\end{aligned}
$$

In terms of z, we can write as follows

$$
\begin{aligned}
\omega'_D &= \Bigg[\Big\{\sigma^2\Psi^{-4q}\Big(-2q^2\Big(\Big[\Big\{\sqrt{6}c\sigma^2\Big(\sqrt{H_0^2\Psi^{2q+2}} - H_0\Psi^\sigma\Big)\Psi^{-2q}\Big\}\{q^2\}^{-1}\Big] \\
&+ 12n^2\Big)\Big(12n^2 - \Big[\Big\{\sigma^2\Big(12H_0^2\Psi^{2q+2} - \sqrt{6}c\Big(\sqrt{H_0^2\Psi^{2q+2}} - H_0\Psi^\sigma\Big)\Big) \\
&\times \Psi^{-2q}\Big\}\{q^2\}^{-1}\Big]\Big)\Big(\Big[\Big\{\Big(12H_0^2\Psi^{2q+2}\psi - \sqrt{6}c\Big(\sqrt{H_0^2\Psi^{2q+2}} - H_0\Psi^\sigma\Big)\Big) \\
&\times \sigma^2\Psi^{-2q}\Big\}\{q^2\}^{-1}\Big] - 12n^2\Big)\Psi^{2q} + 12H_0^2\sigma^2\Big(\Big[\Big\{\sqrt{6}c\sigma^2\Big(\sqrt{H_0^2\Psi^{2q+2}} \\
&- H_0\Psi^\sigma\Big)\Psi^{-2q}\Big\}\{q^2\}^{-1}\Big] + 12n^2\Big)\Big(\Big[\Big\{\sigma^2\Psi^{-2q}\Big(12H_0^2\Psi^{2q+2}\psi - \sqrt{6}c \\
&\times \Big(\sqrt{H_0^2\Psi^{2q+2}} - H_0\Psi^\sigma\Big)\Big)\Big\}\{q^2\}^{-1}\Big] - 12n^2\Big)\Big(\frac{c}{2\sqrt{6}\sqrt{H_0^2\Psi^{2q+2}}} - 2\Big)
\end{aligned}
$$

14

$$\times \quad \Psi^{2q+2}\left(\left[\left\{\left(\sqrt{H_0^2\Psi^{2q+2}}-H_0\Psi^\sigma\right)\sqrt{6}c\sigma^2\Psi^{-2q}\right\}\{q^2\}^{-1}\right]+12n^2\right)$$

$$- \quad 12\sigma^2 H_0^2\left(12n^2-\left[\left\{\left(12H_0^2\Psi^{2q+2}-\sqrt{6}c\left(\sqrt{H_0^2\Psi^{2q+2}}-H_0\Psi^\sigma\right)\right)\right.\right.\right.$$

$$\times \quad \Psi^{-2q}\sigma^2\right\}\{q^2\}^{-1}\left]\right)\left(2\psi-\frac{c}{2\sqrt{6}\sqrt{H_0^2\Psi^{2q+2}}}\right)\Psi^{2q+2}+\left(\left[\left\{\left(12H_0^2\right.\right.\right.\right.$$

$$\times \quad \Psi^{2q+2}\psi-\sqrt{6}c\left(\sqrt{H_0^2\Psi^{2q+2}}-H_0\Psi^\sigma\right)\right)\sigma^2\Psi^{-2q}\right\}\{q^2\}^{-1}\left]-12n^2\right)$$

$$\times \quad \sqrt{6}c\sigma^2\left(12n^2-\left[\left\{\Psi^{-2q}\sigma^2\left(12H_0^2\Psi^{2q+2}-\left(\sqrt{H_0^2\Psi^{2q+2}}-H_0\Psi^\sigma\right)\right.\right.\right.\right.$$

$$\times \quad \left.\sqrt{6}c\right)\right\}\{q^2\}^{-1}\left]\right)\sqrt{H_0^2\Psi^{2q+2}}\right\}\left\{2q^4\left(\left[\left\{c\sigma^2\left(\sqrt{H_0^2\Psi^{2q+2}}-H_0\Psi^\sigma\right)\right.\right.\right.\right.$$

$$\times \quad \sqrt{6}\Psi^{-2q}\right\}\{q^2\}^{-1}\left]+12n^2\right)^2\left(\left[\left\{\left(12H_0^2\Psi^{2q+2}-\sqrt{6}c\left(\sqrt{H_0^2\Psi^{2q+2}}\right.\right.\right.\right.\right.$$

$$- \quad \left.\left.H_0\Psi^\sigma\right)\right)\Psi^{-2q}\sigma^2\right\}\{q^2\}^{-1}\left]-12n^2\right)^2\right\}^{-1}\right].$$

Figure **4** shows how the freezing region is calculated for different values of ψ and n, where $\omega_D < 0$, $\omega'_D < 0$. This indicates an acceleration in cosmic expansion at higher rates in this context.

4.3 The $(r-s)$-Plane

One way to explore the the universe's dynamics from a cosmological viewpoint is through statefinder (r,s) analysis [37]. Understanding various DE models require this essential approach. Trajectories are classified as part of the quintessence and phantom phases if they exist in the region $(r < 1; s > 0)$, while the Chaplygin gas models manifested when $(r > 1; s < 0)$. The flat universe is characterized by these specific parameters

$$r = \frac{\dddot{a}}{aH^3}, \quad s = \frac{r-1}{3(q-\frac{1}{2})}.$$

The cosmos consists of two distinct parts of the EoS parameters, ω_D and ω_m, representing exotic energy and ordinary matter, respectively. The values (r,s) are defined as

$$r = 1 + \frac{9\omega_D}{2}\Omega_D(1+\omega_D) - \frac{3\omega'_D}{2H}\Omega_D, \quad s = 1 + \omega_D - \frac{\omega'_D}{3\omega_D H}.$$

15
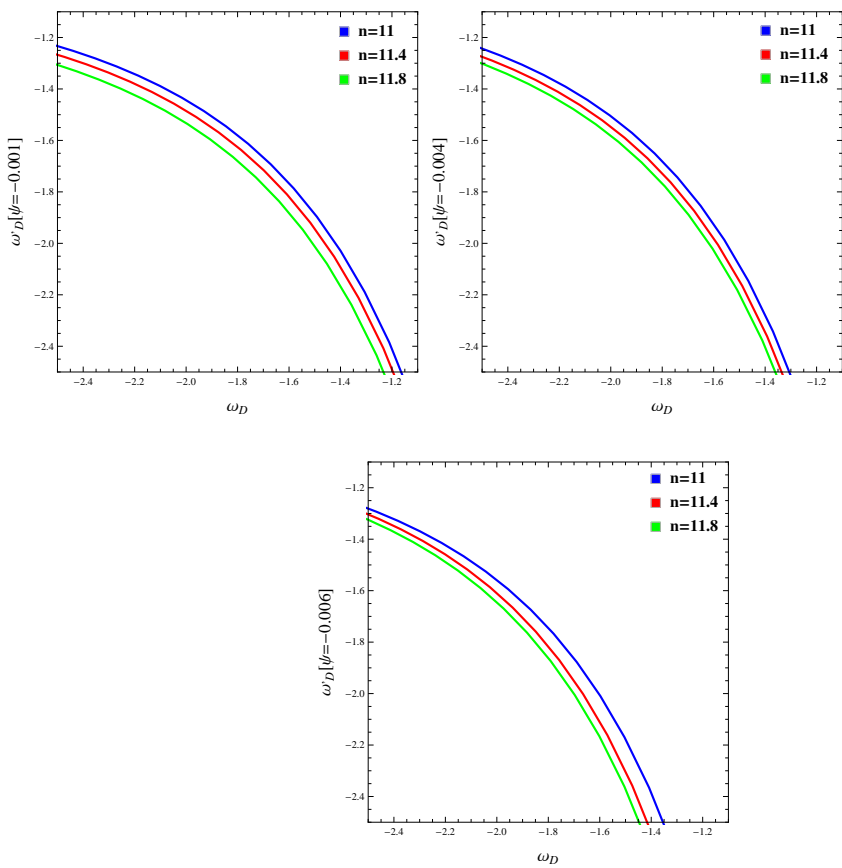
Figure 4: Graphs of ω'_D versus ω_D.

These parameters for the NADE $f(\mathcal{Q})$ gravity turn out to be

$$
\begin{aligned}
r &= \Bigg[\Big\{-24\eta^4 n^2\Big(3c^2\Big(6H^2\Big(3\sqrt{6}-9\mathcal{Q}^{3/2}-4\sqrt{\mathcal{Q}}\Big)+\Big(9\sqrt{6}\mathcal{Q}^2-15\sqrt{\mathcal{Q}}\\
&\quad+ 4\sqrt{6}\mathcal{Q}\Big)2H-4\mathcal{Q}^{3/2}-9\mathcal{Q}^{5/2}+2\sqrt{6}\mathcal{Q}\Big)+2c\Big(-H\Big(9\sqrt{6}\mathcal{Q}^{3/2}(2\psi+1)\\
&\quad- 72\psi+16\sqrt{6}\sqrt{\mathcal{Q}}\Big)+9\mathcal{Q}^2(2\psi+1)-9\sqrt{6}\sqrt{\mathcal{Q}}\psi+16\mathcal{Q}\Big)\mathcal{Q}+12\sqrt{6}\mathcal{Q}^2\psi\\
&\quad- 16\mathcal{Q}^{5/2}\Big)+\eta^6\Big(c^3\Big(-12H^3\Big(9\sqrt{6}\mathcal{Q}^{3/2}+4\sqrt{6}\sqrt{\mathcal{Q}}-18\Big)-\Big(5\sqrt{6}\sqrt{\mathcal{Q}}\\
&\quad- 8\mathcal{Q}-18\mathcal{Q}^2\Big)18H^2-6H\Big(9\sqrt{6}\mathcal{Q}^{3/2}+4\sqrt{6}\sqrt{\mathcal{Q}}-12\Big)\mathcal{Q}-3\sqrt{6}\mathcal{Q}^{3/2}\\
&\quad+ 18\mathcal{Q}^3+8\mathcal{Q}^2\Big)-2c^2\mathcal{Q}\Big(6H^2\Big(9\mathcal{Q}^{3/2}(2\psi+1)+16\sqrt{\mathcal{Q}}-12\sqrt{6}\psi\Big)-2H\\
&\quad\times \Big(16\sqrt{6}\mathcal{Q}-54\sqrt{\mathcal{Q}}\psi+9\sqrt{6}\mathcal{Q}^2(2\psi+1)\Big)+9\mathcal{Q}^{5/2}(2\psi+1)+16\mathcal{Q}^{3/2}-6\\
&\quad\times \sqrt{6}\mathcal{Q}\psi\Big)+4c\mathcal{Q}^2\Big(36H\psi-8\sqrt{6}H\sqrt{\mathcal{Q}}-3\sqrt{6}\sqrt{\mathcal{Q}}\psi+8\mathcal{Q}\Big)+72\mathcal{Q}^{9/2}\psi^2\Big)\\
&\quad- 144\eta^2 n^4\Big(3c\Big(2H\Big(9\sqrt{6}\mathcal{Q}^{3/2}+4\sqrt{6}\sqrt{\mathcal{Q}}-18\Big)-18\mathcal{Q}^2-8\mathcal{Q}+5\sqrt{6}\sqrt{\mathcal{Q}}\Big)\\
&\quad+ 18\mathcal{Q}^{\frac{5}{2}}(2\psi+1)-24\sqrt{6}\mathcal{Q}\psi+32\mathcal{Q}^{\frac{3}{2}}\Big)-3456n^6\Big(3\sqrt{6}-9\mathcal{Q}^{\frac{3}{2}}-4\sqrt{\mathcal{Q}}\Big)\Big\}\\
&\quad\times \Big\{\sqrt{\mathcal{Q}}\big(c\eta^2(\sqrt{\mathcal{Q}}-\sqrt{6}H)+12n^2\big)\big(\eta^2(\sqrt{6}cH-c\sqrt{\mathcal{Q}}+\mathcal{Q})-12n^2\big)^2\Big\}^{-1}\Bigg],\\[4pt]
s &= \Bigg[\Big\{-24\eta^4 n^2\Big(c^2\Big(18H^2\Big(\sqrt{6}-3\mathcal{Q}^{\frac{3}{2}}\Big)+6H\Big(3\sqrt{6}\mathcal{Q}^2-5\sqrt{\mathcal{Q}}\Big)+\sqrt{6}\mathcal{Q}\\
&\quad- 9\mathcal{Q}^{\frac{5}{2}}\Big)+6c\Big(-H\Big(\sqrt{6}\mathcal{Q}^{\frac{5}{2}}(2\psi+1)-8\mathcal{Q}\psi\Big)-\sqrt{6}\mathcal{Q}^{\frac{3}{2}}\psi+\mathcal{Q}^3(2\psi+1)\Big)\\
&\quad+ 4\sqrt{6}\mathcal{Q}^2\psi\Big)+\eta^6\Big(c^3\Big(-36H^3\Big(\sqrt{6}\mathcal{Q}^{3/2}-2\Big)-6H^2\Big(5\sqrt{6}\sqrt{\mathcal{Q}}-18\mathcal{Q}^2\Big)\\
&\quad- 6H\Big(3\sqrt{6}\mathcal{Q}^{\frac{3}{2}}-4\Big)\mathcal{Q}-\sqrt{6}\mathcal{Q}^{\frac{3}{2}}+6\mathcal{Q}^3\Big)-2c^2\mathcal{Q}\Big(\Big(\mathcal{Q}^{\frac{3}{2}}(6\psi+3)-4\sqrt{6}\psi\Big)\\
&\quad\times 6H^2-6H\Big(\sqrt{6}\mathcal{Q}^2(2\psi+1)-6\sqrt{\mathcal{Q}}\psi\Big)+\mathcal{Q}^{\frac{5}{2}}(6\psi+3)-2\sqrt{6}\mathcal{Q}\psi\Big)+c
\end{aligned}
$$

$$\times \quad \left(48H\mathcal{Q}^2\psi - 4\sqrt{6}\mathcal{Q}^{5/2}\psi\right) + 24\mathcal{Q}^{9/2}\psi^2\right) - 144\left(\left(18H\left(\sqrt{6}\mathcal{Q}^{3/2} - 2\right)\right.\right.$$

$$- \quad 18\mathcal{Q}^2 + 5\sqrt{6}\sqrt{\mathcal{Q}}\right)c + 6\mathcal{Q}^{5/2}(2\psi + 1) - 8\sqrt{6}\mathcal{Q}\psi\right)\eta^2 n^4 - 3456n^6\left(\sqrt{6}\right.$$

$$- \quad 3\mathcal{Q}^{3/2}\right)\right\}\left\{6\mathcal{Q}^{3/2}\left(c\eta^2\left(\sqrt{\mathcal{Q}} - \sqrt{6}H\right) + 12n^2\right)\left(\eta^2\left(\sqrt{6}cH - c\sqrt{\mathcal{Q}}\right.\right.\right.$$

$$+ \quad 2\mathcal{Q}\right) - 12n^2\right)\left(\eta^2\left(\sqrt{6}cH - c\sqrt{\mathcal{Q}} + 2\mathcal{Q}\psi\right) - 12n^2\right)\right\}^{-1}\bigg],$$

while in the context of z, we get

$$r \quad = \quad \left[\left\{-3456\sqrt{6}n^6\left(3 - 54\left(H_0^2\Psi^{2q+2}\right)^{3/2} - 4\sqrt{H_0^2\Psi^{2q+2}}\right) - \left[\left\{432n^4\sigma^2\right.\right.\right.\right.$$

$$\times \quad \Psi^{-2q}\left(64\sqrt{6}\left(H_0^2\Psi^{2q+2}\right)^{3/2} + 216\sqrt{6}(2\psi + 1)\left(H_0^2\Psi^{2q+2}\right)^{5/2} + \left(\left(54\right.\right.\right.$$

$$\times \quad \left(H_0^2\Psi^{2q+2}\right)^{3/2} + 4\sqrt{H_0^2\Psi^{2q+2}} - 3\right)2H_0\Psi^\sigma - 8H_0^2\Psi^{2q+2} - 108H_0^4\Psi^{4q+4}$$

$$+ \quad 5\sqrt{H_0^2\Psi^{2q+2}}\right)6c - 48\sqrt{6}H_0^2\Psi^{2q+2}\psi\right)\right\}\left\{q^2\right\}^{-1}\right] + \left[\left\{\sigma^6\Psi^{-6q}\left(93312\sqrt{6}\psi^2\right.\right.\right.$$

$$\times \quad \left(H_0^2\Psi^{2q+2}\right)^{9/2} + 6c^3\left(-18\left(H_0^2\Psi^{2q+2}\right)^{3/2} + 48H_0^4\Psi^{4q+4} + 648H_0^6\Psi^{6q+6}\right.$$

$$- \quad 3H_0^2\left(30\sqrt{H_0^2\Psi^{2q+2}} - 48H_0^2\Psi^{2q+2} - 648H_0^4\Psi^{4q+4}\right)\Psi^{2q+2} - 72H_0^3\Psi^{3q+3}$$

$$\times \quad \left(27\left(H_0^2\Psi^{2q+2}\right)^{3/2} - 1 + 2\sqrt{H_0^2\Psi^{2q+2}}\right) - 12H_0^3\Psi^{3q+3}\left(54\left(H_0^2\Psi^{2q+2}\right)^{3/2}\right.$$

$$+ \quad 4\sqrt{H_0^2\Psi^{2q+2}} - 3\right)\right) + 864H_0^4c\left(6H_0\psi\Psi^\sigma - 8H_0\sqrt{H_0^2\Psi^{2q+2}}\Psi^\sigma + 8H_0^2\Psi^{2q+2}\right.$$

$$- \quad 3\sqrt{H_0^2\Psi^{2q+2}}\psi\right)\Psi^{4q+4} - 144\sqrt{6}c^2H_0^2\Psi^{2q+2}\left(8\left(H_0^2\Psi^{2q+2}\right)^{3/2} + 27(2\psi + 1)\right.$$

$$\times \quad \left(H_0^2\Psi^{2q+2}\right)^{5/2} - 3H_0^2\Psi^{2q+2}\psi - H_0\Psi^\sigma\left(16H_0^2\Psi^{2q+2} + 54H_0^4(2\psi + 1)\Psi^{4q+4}\right.$$

$$- \quad 9\sqrt{H_0^2\Psi^{2q+2}}\psi\right) + H_0^2\Psi^{2q+2}\left(27(2\psi + 1)\left(H_0^2\Psi^{2q+2}\right)^{3/2} + 8\sqrt{H_0^2\Psi^{2q+2}}\right.$$

$$
\begin{aligned}
&- \left. 6\psi\right)\Big)\Big)\Big\}\{q^6\}^{-1}\right] - \left[\Big\{144n^2\sigma^4\Psi^{-4q}\Big(-96\sqrt{6}\Big(H_0^2\Psi^{2q+2}\Big)^{5/2} + 3\sqrt{6}c^2 \right.\\
&\times \ \left(-4\Big(H_0^2\Psi^{2q+2}\Big)^{3/2} - 54\Big(H_0^2\Psi^{2q+2}\Big)^{5/2} + 2H_0^2\Psi^{2q+2} + H_0\Psi^\sigma\Big(8H_0^2\Psi^{2q+2} \right.\\
&+ \ \left. 108H_0^4\Psi^{4q+4} - 5\sqrt{H_0^2\Psi^{2q+2}}\Big) + \Big(3 - 54\Big(H_0^2\Psi^{2q+2}\Big)^{3/2} - 4\sqrt{H_0^2\Psi^{2q+2}}\Big)\right.\\
&\times \ \left. H_0^2\Psi^{2q+2}\right) + 72\sqrt{6}H_0^4\Psi^{4q+4}\psi + 2cH_0^2\Psi^{2q+2}\Big(96H_0^2\Psi^{2q+2} - \Big(324(2\psi + 1)\right.\\
&\times \ \left. \Big(H_0^2\Psi^{2q+2}\Big)^{3/2} + 96\sqrt{H_0^2\Psi^{2q+2}} - 72\psi\Big)H_0\Psi^\sigma + 324H_0^4(2\psi + 1)\Psi^{4q+4}\right.\\
&\times \ \left. \left. \Psi^{-2q}\Big\}\{q^2\}^{-1}\right] - 54\sqrt{H_0^2\Psi^{2q+2}}\psi\Big)\Big)\Big\}\{q^4\}^{-1}\right]\right\}\left\{\sqrt{H_0^2\Psi^{2q+2}}\Big(\left[\Big\{\sqrt{6}c\sigma^2\right.\\
&\times \ \left(\sqrt{H_0^2\Psi^{2q+2}} - H_0\Psi^\sigma\Big) + 12n^2\right)8\sqrt{6}\Big(\left[\Big\{\sigma^2\Psi^{-2q}\Big(12H_0^2\Psi^{2q+2} - \sqrt{6}c\right.\\
&\times \ \left. \left. \left. \Big(\sqrt{H_0^2\Psi^{2q+2}} - H_0\Psi^\sigma\Big)\Big)\Big\}\{q^2\}^{-1}\right] - 12n^2\Big)^2\Big\}^{-1}\right].
\end{aligned}
$$

$$
\begin{aligned}
s \ = \ &\left[\Big\{-576\sqrt{6}n^6\Big(1 - 18\Big(H_0^2\Psi^{2q+2}\Big)^{\frac{3}{2}}\Big) - \left[\Big\{24n^4\sigma^2\Psi^{-2q}\Big(216\sqrt{6}(2\psi + 1)\right.\right.\\
&\times \ \left(H_0^2\Psi^{2q+2}\Big)^{\frac{5}{2}} + c\Big(18H_0\Big(36\Big(H_0^2\Psi^{2q+2}\Big)^{\frac{3}{2}} - 2\Big)\Psi^\sigma - 648H_0^4\Psi^{4q+4} + 30\right.\\
&\times \ \left. \sqrt{H_0^2\Psi^{2q+2}}\Big) - 48\sqrt{6}H_0^2\Psi^{2q+2}\psi\Big)\Big\}\{q^2\}^{-1}\right] - \left[\Big\{24n^2\sigma^4\Psi^{-4q}\Big(\sqrt{6}c^2H_0\right.\\
&\times \ \left(108H_0^3\Psi^{3q+3} + 5\Big)\Big(H_0\Psi^\sigma - \sqrt{H_0^2\Psi^{2q+2}}\Big)\Psi^\sigma + 24\sqrt{6}H_0^4\psi\Psi^{4q+4} + c\right.\\
&\times \ \left(216H_0^6\Psi^{6q+6}(2\psi + 1) - 36\psi\Big(H_0^2\Psi^{2q+2}\Big)^{\frac{3}{2}} - H_0\Psi^\sigma\Big(216\Big(H_0^2\Psi^{2q+2}\Big)^{\frac{5}{2}}\right.\\
&\times \ \left. \left. (2\psi + 1) - 48H_0^2\Psi^{2q+2}\psi\Big)\Big)\Big)\Big\}\{q^4\}^{-1}\right] + \left[\Big\{\sigma^6\Big(84\sqrt{6}\psi^2\Big(H_0^2\Psi^{2q+2}\Big)^{\frac{9}{2}}\right.\\
&+ \ c^3\Big(216H_0^6\Psi^{6q+6} - 6\Big(H_0^2\Psi^{2q+2}\Big)^{\frac{3}{2}} - \Big(30\sqrt{H_0^2\Psi^{2q+2}} - 648H_0^4\Psi^{4q+4}\Big)\\
&\times \ H_0^2\Psi^{2q+2} - 6H_0^3\Psi^{3q+3}\big(36\big(H_0^2\Psi^{2q+2}\big)^{\frac{3}{2}} - 2\big) - \Big(108\big(H_0^2\Psi^{2q+2}\big)^{\frac{3}{2}} - 4\Big)
\end{aligned}
$$
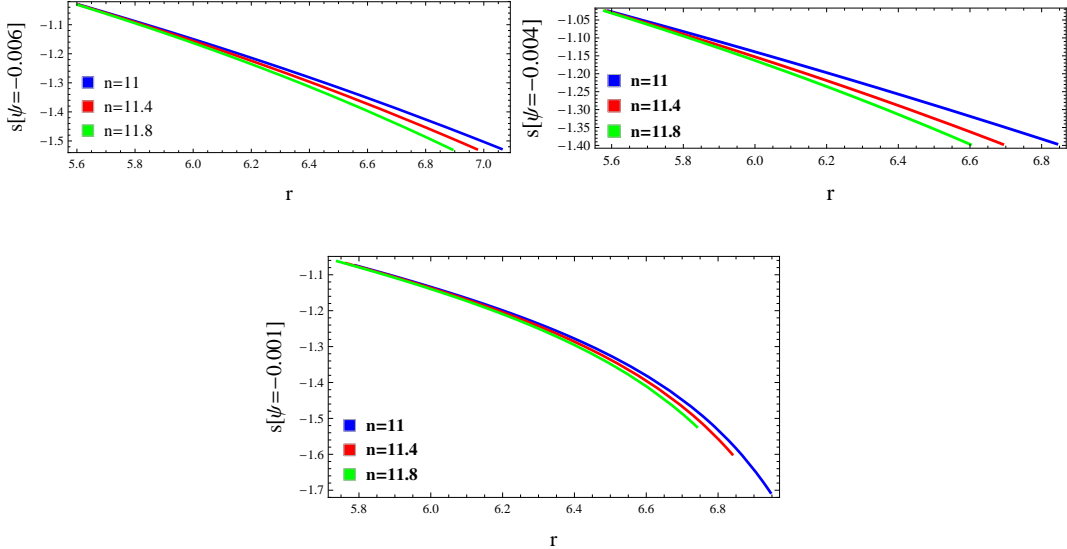
Figure 5: Graphs of s versus r.

$$\times \quad 6H_0^3\Psi^{3q+3}\Big) + 144c\Big(2H_0^5\Psi^{5q+5} - \Big(H_0^2\Psi^{2q+2}\Big)^{\frac{5}{2}}\Big)\psi - 24\sqrt{6}c^2H_0^2\Psi^{2q+2}$$

$$\times \quad \Big(3(6\psi+3)\Big(H_0^2\Psi^{2q+2}\Big)^{5/2} - H_0^2\Psi^{2q+2}\psi - 3H_0\Psi^\sigma\Big(6H_0^4\Psi^{4q+4}(2\psi+1)$$

$$- \quad \sqrt{H_0^2\Psi^{2q+2}}\psi\Big) + H_0^2\Psi^{2q+2}\Big(3\Big(H_0^2\Psi^{2q+2}\Big)^{\frac{3}{2}}(6\psi+3) - 2\psi\Big)\Big)\Big)\Psi^{-6q}\Big\}$$

$$\times \quad \{q^6\}^{-1}\Big]\Big\}\Big\{6\sqrt{6}\big(H_0^2\Psi^{2q+2}\big)^{\frac{3}{2}}\Big(\Big[\Big\{\sqrt{6}c\sigma^2\Big(\sqrt{H_0^2\Psi^{2q+2}} - H_0\Psi^\sigma\Big)\Psi^{-2q}\Big\}$$

$$\times \quad \{q^2\}^{-1}\Big] + 12n^2\Big)\Big(\Big[\Big\{\sigma^2\Big(12H_0^2\Psi^{2q+2} - \sqrt{6}c\Big(\sqrt{H_0^2\Psi^{2q+2}} - H_0\Psi^\sigma\Big)\Big)$$

$$\times \quad \Psi^{-2q}\Big\}\{q^2\}^{-1}\Big] - 12n^2\Big)\Big(\Big[\Big\{\sigma^2\Psi^{-2q}\Big(12H_0^2\Psi^{2q+2}\psi - \sqrt{6}c\Big(\sqrt{H_0^2\Psi^{2q+2}}$$

$$- \quad H_0\Psi^\sigma\Big)\Big)\Big\}\{q^2\}^{-1}\Big] - 12n^2\Big)\Big\}^{-1}\Big].$$

For all values of n and ψ, Figure **5** depicts the behavior of the $(r-s)$-plane as the Chaplygin gas model.

4.4 The Squared Speed of Sound Parameter

The squared speed of sound parameter can be expressed as

$$\nu_s^2 = \frac{P_{GGDE}}{\rho'_{GGDE}}\omega'_{GGDE} + \omega_{GGDE}. \tag{29}$$

The signature of ν_s^2 is essential in analyzing the stability of the reconstructed NADE model. The presence of a positive ν_s^2 indicates stability, while a negative ν_s^2 denotes instability in the model. The corresponding ν_s^2 is given as

$$
\begin{aligned}
\nu_s^2 &= \left[\left\{\left(c\eta^2\left(Q(2e-Q)+6H^2Q-H\right)-12n^2Q^{3/2}\right)\left(-\left[\left\{\left(\eta^2\left(\sqrt{6}cH\right.\right.\right.\right.\right.\right. \\
&\quad - c\sqrt{Q}+2Q\psi\right)-12n^2\right)\eta^2\right\}\left\{\left(c\eta^2(\sqrt{Q}-\sqrt{6}H)+12n^2\right)\left(\eta^2\left((\sqrt{Q}\right.\right.\right. \\
&\quad \left.\left.\left.\left.- \sqrt{6}H)c-2Q\right)+12n^2\right)\right\}^{-1}\right]+\left[\left\{c\sqrt{Q}\left(\eta^2\left(\sqrt{6}cH-c\sqrt{Q}+2Q\psi\right)\right.\right.\right. \\
&\quad \left.\left.- 12n^2\right)\eta^4\right\}\left\{2\left(c\eta^2(\sqrt{Q}-\sqrt{6}H)+12n^2\right)^2\left(\eta^2\left(c(\sqrt{Q}-\sqrt{6}H)-2\right.\right.\right. \\
&\quad \left.\left.\left.\times~Q\right)+12n^2\right)\right\}^{-1}\right]+\left[\left\{\eta^4Q\left(\frac{c}{2\sqrt{Q}}-2\right)\left(\eta^2\left(\sqrt{6}cH-c\sqrt{Q}+2Q\psi\right)\right.\right.\right. \\
&\quad \left.\left.- 12n^2\right)\right\}\left\{\left(c\eta^2\left(\sqrt{Q}-\sqrt{6}H\right)+12n^2\right)\left(\eta^2\left(c\left(\sqrt{Q}-\sqrt{6}H\right)-2Q\right)\right.\right. \\
&\quad \left.\left.+~12n^2\right)\right\}^{-1}\right]-\left[\left\{\eta^4Q\left(2\psi-\frac{c}{2\sqrt{Q}}\right)\right\}\left\{\left(c\eta^2\left(\sqrt{Q}-\sqrt{6}H\right)+12n^2\right)\right.\right. \\
&\quad \left.\times~\left(\eta^2\left(c(\sqrt{Q}-\sqrt{6}H)-2Q\right)+12n^2\right)\right\}^{-1}\right]\right)\right\}\left\{\left[\left\{c(2\eta^2Q^{3/2})\right\}\left\{\sqrt{Q}\right.\right.\right. \\
&\quad \left.\left.\times~4\right\}^{-1}\right]\right\}^{-1}\right]-\left[\left\{\eta^2Q\left(\eta^2\left(\sqrt{6}cH-c\sqrt{Q}+2Q\psi\right)-12n^2\right)\right\}\left\{\left(c\eta^2\right.\right.\right. \\
&\quad \left.\times~\left(\sqrt{Q}-\sqrt{6}H\right)+12n^2\right)\left(\eta^2\left(c\left(\sqrt{Q}-\sqrt{6}H\right)-2Q\right)+12n^2\right)\right\}^{-1}\right],
\end{aligned}
$$

while in the context of the z, it can be observed that

$$
\nu_s^2 = \left[\left\{\left[\left\{\Psi^{-4q}\left(-72\sqrt{6}n^2\left(H_0^2\Psi^{2q+2}\right)^{3/2}-\left[\left\{cH_0\left(12H_0^2\Psi^{3q+3}+1\right)\sigma^2\right.\right.\right.\right.\right.\right.\right.
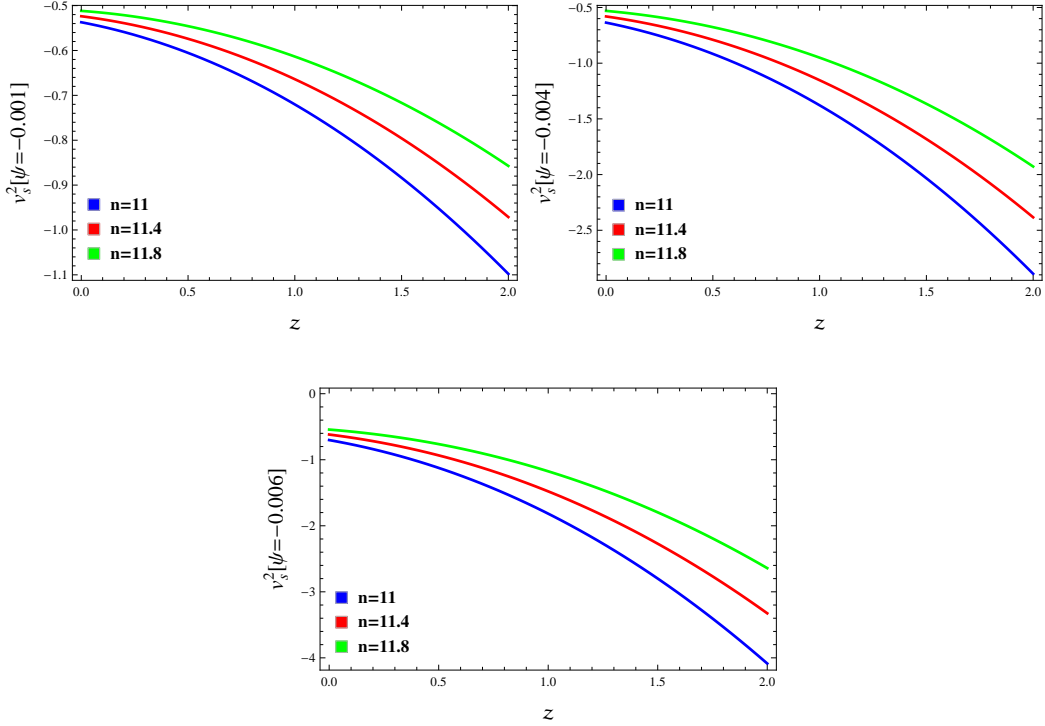$$

21

$$\times \quad \Psi^{1-q}\Big\}\{q^2\}^{-1}\Big]\Big)\Big(-2q^2\Big(\Big[\Big\{\sqrt{6}c\sigma^2\Big(\sqrt{H_0^2\Psi^{2q+2}}-H_0\Psi^\sigma\Big)\Psi^{-2q}\Big\}$$

$$\times \quad \{q^2\}^{-1}\Big]+12n^2\Big)\Big(12n^2-\Big[\Big\{\sigma^2\Psi^{-2q}\Big(12H_0^2\Psi^{2q+2}-\Big(\sqrt{H_0^2\Psi^{2q+2}}$$

$$- \quad H_0\Psi^\sigma\Big)\sqrt{6}c\Big)\Big\}\{q^2\}^{-1}\Big]\Big)\Big(\Big[\Big\{\sigma^2\Psi^{-2q}\Big(12H_0^2\Psi^{2q+2}\psi-\Big(\sqrt{H_0^2\Psi^{2q+2}}$$

$$- \quad H_0\Psi^\sigma\Big)\sqrt{6}c\Big)\Big\}\{q^2\}^{-1}\Big]-12n^2\Big)\Psi^{2q}+12H_0^2\sigma^2\Big(\Big[\Big\{\sqrt{6}c\Big(\sqrt{H_0^2\Psi^{2q+2}}$$

$$- \quad H_0\Psi^\sigma\Big)\sigma^2\Psi^{-2q}\Big\}\{q^2\}^{-1}\Big]+12n^2\Big)\Big(\Big[\Big\{\sigma^2\Psi^{-2q}\Big(12H_0^2\Psi^{2q+2}\psi-\sqrt{6}c$$

$$\times \quad \Big(\sqrt{H_0^2\Psi^{2q+2}}-H_0\Psi^\sigma\Big)\Big)\Big\}\{q^2\}^{-1}\Big]-12n^2\Big)\Big(\Big[\Big\{2\sqrt{6}\sqrt{H_0^2\Psi^{2q+2}}\Big\}^{-1}$$

$$\times \quad \{c\}\Big]-2\Big)\Psi^{2q+2}-12H_0^2\sigma^2\Big(\Big[\Big\{\sqrt{6}c\sigma^2\Big(\sqrt{H_0^2\Psi^{2q+2}}-H_0\Psi^\sigma\Big)\Psi^{-2q}\Big\}$$

$$\times \quad \{q^2\}^{-1}\Big]+12n^2\Big)\Big(12n^2-\Big[\Big\{\sigma^2\Psi^{-2q}\Big(12H_0^2\Psi^{2q+2}-\sqrt{6}c(\sqrt{H_0^2\Psi^{2q+2}}$$

$$- \quad H_0\Psi^\sigma)\Big)\Big\}\{q^2\}^{-1}\Big]\Big)\Big(2\psi-\Big[\{c\}\Big\{2\sqrt{6}\sqrt{H_0^2\Psi^{2q+2}}\Big\}^{-1}\Big]\Big)\Psi^{2q+2}+\sqrt{6}$$

$$\times \quad c\sigma^2\Big(\Big[\Big\{\sigma^2\Psi^{-2q}\Big(H_0^2\Psi^{2q+2}\psi-\sqrt{6}c\Big(\sqrt{H_0^2\Psi^{2q+2}}-H_0\Psi^\sigma\Big)\Big)\Big\}\{q^2\}^{-1}\Big]$$

$$- \quad 12n^2\Big)\Big(12n^2-\Big[\Big\{\sigma^2\Psi^{-2q}\Big(H_0^2\Psi^{2q+2}-\sqrt{6}c\Big(\sqrt{H_0^2\Psi^{2q+2}}-H_0\Psi^\sigma\Big)\Big)\Big\}$$

$$\times \quad \{q^2\}^{-1}\Big]\Big)\sqrt{H_0^2\Psi^{2q+2}}\Big)\Big\}\Big\{c\Big(\Big[\Big\{\sigma^2\Psi^{-2q}\Big(H_0^2\Psi^{2q+2}-\sqrt{6}c\Big(\sqrt{H_0^2\Psi^{2q+2}}$$

$$- \quad H_0\Psi^\sigma\Big)\Big)\Big\}\{q^2\}^{-1}\Big]-12n^2\Big)^2\Big\}^{-1}\Big]-\Big[\Big\{H_0^4\sigma^2\Psi^4\Big(\Big[\Big\{\sqrt{6}c\Big(\sqrt{H_0^2\Psi^{2q+2}}$$

$$- \quad H_0\Psi^\sigma\Big)\sigma^2\Psi^{-2q}\Big\}\{q^2\}^{-1}\Big]+12n^2\Big)\Big(\Big[\Big\{\sigma^2\Big(12H_0^2\Psi^{2q+2}\psi-\Big(\sqrt{H_0^2\Psi^{2q+2}}$$

$$- \quad H_0\Psi^\sigma\Big)\sqrt{6}c\Big)\Psi^{-2q}\Big\}\{q^2\}^{-1}\Big]-12n^2\Big)\Big\}\Big\{12n^2-\Big[\Big\{\sigma^2\Psi^{-2q}\Big(12H_0^2\Psi^{2q+2}$$

$$- \quad \sqrt{6}c\Big(\sqrt{H_0^2\Psi^{2q+2}}-H_0\Psi^\sigma\Big)\Big)\Big\}\{q^2\}^{-1}\Big]\Big\}\Big\{6H_0^2q^2\Psi^2\Big(\Big[\Big\{\sigma^2\Big(\sqrt{H_0^2\Psi^{2q+2}}$$

Figure 6: Graphs of ν_s^2 versus z.

$$\left. - \quad H_0 \Psi^\sigma \right) \sqrt{6} c \Psi^{-2q} \Big\} \big\{ q^2 \big\}^{-1} \bigg] + 12 n^2 \Big)^2 \Big\}^{-1} \bigg]. \tag{30}$$

Several studies have investigated this aspect for different DE models. For instance, Setare [38] examined the interacting HDE model with the Chaplygin gas and found that both models exhibit instability. Kim et al. [39] showed that the NADE model is always negative, indicating its instability. Figure **6** shows that the NADE $f(\mathcal{Q})$ model is unstable for all values of n and ψ, as the ν_s^2 remains negative throughout the evolution of the universe. This aligns with the previous studies, showing that the $f(\mathcal{Q})$ model faces similar instability challenges in the literature.

5 Conclusions

In this paper, we have examined the NADE model in the $f(\mathcal{Q})$ gravity. Initially, we have utilized the correspondence scheme to reconstruct the NADE $f(\mathcal{Q})$ gravity model. We have applied the FRW model with a power-law expression for the scale factor in the interacting scenario. We have assumed that the densities of NADE and $f(\mathcal{Q})$ gravity are equal to find NADE $f(\mathcal{Q})$ gravity model. We have graphically analyzed the behavior of NADE model for three distinct values of $n = 11, 11.4, 11.8$. We have analyzed the EoS, $(\omega_D - \omega'_D)$ and $(r - s)$ planes. The ν_s^2 is employed to analyze the stability of the interacting NADE $f(\mathcal{Q})$ gravity model. The key findings are outlined as follows.

- The NADE $f(\mathcal{Q})$ gravity model shows an increasing pattern for both z and $\mathcal{Q}$ with selected values of n, indicating the realistic nature of the reconstructed model (Figure **1**).

- The energy density demonstrates a positive trend, while the pressure shows negative behavior for all values of n. These observations align with the typical features of DE (Figure **2**).

- In the later stages of evolution, it is observed that ω_D behaves as the quintessence-like characteristic for power-law form using various values of n and ψ (Figure **3**). It is noted that the rate of evolution of the energy density could be sufficiently slow at present time resolving the coincidence problem.

- The evolutionary pattern of the $(\omega_D$-$\omega'_D)$-plane shows the region where freezing occurs for chossen values of ψ and n (Figure **4**). This indicates that the NADE $f(\mathcal{Q})$ gravity suggests a more rapid expansion of the universe.

- The $(r - s)$-plane depicts the Chaplygin gas model for various values of ψ and n (Figure **5**).

- We have determined that the ν_s^2 is negative, indicating instability for selected values of ψ and n in the NADE $f(\mathcal{Q})$ gravity (Figure **6**).

Jawad et al. [40] examined the NADE model in the $f(\mathcal{G})$ gravity ($\mathcal{G}$ is the Gauss-Bonnet invariant) to analyze the expansion of the universe and

assessed the stability of the model. They found that NADE $f(\mathcal{G})$ model demonstrated a graphically decreasing behavior. The reconstructed NADE $f(\mathcal{Q})$ model shows a graphical increasing trend. Both models are unstable as the universe evolves and both show a quintessence region for acceleration observed through the EoS. The key concept in theoretical progressions involves higher-order gravitational theories that incorporate anti-gravity phenomena due to higher-order curvature terms. It is important to mention here that the $f(\mathcal{Q})$ theory is better suited for addressing the above mentioned problem as compared to $f(\mathcal{G})$ since the field equations of $f(\mathcal{Q})$ gravity are second order, whereas the field equations of $f(\mathcal{G})$ gravity are fourth order.

Data Availability Statement: No data was used for the research described in this paper.

References

[1] Riess A.G. et al.: Astron. J. **116**(1998)1009; Perlmutter S. et al.: Astrophys. J. **517**(1999)565.

[2] Nojiri, S. and Odintsov, S.D.: Gen. Relativ. Gravit. **38**(2006)1285.

[3] Cai, R.G.: Phys. Lett. B **657**(2007)228.

[4] Wei, H. and Cai, R.G.: Phys. Lett. B **660**(2008)113.

[5] Wei, H. and Cai, R.G.: Phys. Lett. B **663**(2008)1.

[6] Setare, M.R.: Astrophys. Space Sci. **326**(2010)27.

[7] Jamil, M. and Saridakis, E.N.: J. Cosmol. Astropart. Phys. **2010**(2010)028.

[8] Li, C.J.L.Z., Jing-Fei, Z. and Xin, Z.: Chin. Phys. B **19**(2010)019802.

[9] Zhang, L. et al.: Int. J. Mod. Phys. D **19**(2010)21.

[10] Houndjo, M.J.S. and Piattella, O.F.: Int. J. Mod. Phys. D **21**(2012)1250024.

[11] Sharif, M. and Jawad, A.: Eur. Phys. J. C **73**(2013)2382.

[12] Fayaz, V. et al.: Astrophys. Space Sci. **353**(2014)301.

[13] Setare, M.R., Felegary, F. and Darabi, F.: Int. J. Mod. Phys. D **26**(2017)1750101.

[14] Sharif, M. and Saba, S.: Chin. J. Phys. **59**(2019)393.

[15] Pourbagher, A. and Amani, A.: Mod. Phys. Lett. A **35**(2020)2050166.

[16] Hehl, F.W. et al.: Rev. Mod. Phys. **48**(1976)393.

[17] Aldrovandi, R. and Pereira, J.G.: *Teleparallel Gravity: An Introduction* (Springer, 2013); Haghani, Z. et al.: J. Cosmol. Astropart. Phys. **10**(2012)061; Haghani, Z. et al.: Phys. Rev. D **88**(2013)044024.

[18] Mol, I.: Adv. Appl. Clifford Algebras **27**(2017)2607; Jiménez, J.B., Heisenberg, L. and Koivisto, T.S.: J. Cosmol. Astropart. Phys. **2018**(2018)039; Gakis, V. et al.: Phys. Rev. D **101**(2020)064024.

[19] Einstein, A.: Sitz. Preuss. Akad. Wiss **217**(1928)224; Hayashi, K. and Shirafuji, T.: Phys. Rev. D **19**(1979)3524.

[20] Jiménez, J.B., Heisenberg, L. and Koivisto, T.: Phys. Rev. D **98**(2018)044048.

[21] Lu, J., Zhao, X. and Chee, G.: Eur. Phys. J. C **79**(2019)530.

[22] Lazkoz, R. et al.: Phys. Rev. D **100**(2019)104027.

[23] Frusciante, N.: Phys. Rev. D **103**(2021)044021.

[24] Mandal, S. and Sahoo, P.K.: Phys. Lett. B **823**(2021)136786.

[25] Myrzakulov, N. et al.: Front. Astron. Space Sci. **9**(2022)902552.

[26] Lymperis, A.: J. Cosmol. Astropart. Phys. **11**(2022)018.

[27] Solanki, R., De, A. and Sahoo, P.K.: Phys. Dark Universe **36**(2022)100996.

[28] Koussour, M. et al.: Prog. Theor. Exp. Phys. **2023**(2023)113E01.

[29] Sharif, M. and Ajmal, M.: Chin. J. Phys. **88**(2024)706; Phys. Scr. **99**(2024)085039.

[30] Sharif, M. and Ajmal, M.: Phys. Dark Universe **46**(2024)101572.

[31] Järv, L. et al.: Phys. Rev. D **97**(2018)124025.

[32] Hehl, F.W. et al.: Phys. Rept. **258**(1995)1.

[33] Cai, R.G. et al.: Phys. Rev. D **86**(2012)023511.

[34] Gadbail, G.N., Mandal, S. and Sahoo, P.K.: Physics **4**(2022)1403.

[35] Feng, C. et al.: Phys. Lett. B **665**(2008)111.

[36] Caldwell, R.R. and Linder, E.V.: Phys. Rev. Lett. **95**(2005)141301.

[37] Sahni, V. et al.: J. Exp. Theor. Phys. Lett. **77**(2003)201.

[38] Setare, M.R.: Phys. Lett. B **654**(2007)1.

[39] Kim, K.Y., Lee, H.W. and Myung, Y.S.: Phys. Lett. B **660**(2008)118.

[40] Jawad, A., Chattopadhyay, S. and Pasqua, A.: Eur. Phys. J. Plus **128**(2013)1.